Drug Design, Development and Therapy

Dovepress
open access to scientific and medical research

Open Access Full Text Article

ORIGINAL RESEARCH

Jujuboside A Regulates Calcium Homeostasis and Structural Plasticity to Alleviate Depression-Like Behavior via Shh Signaling in Immature Neurons

Ziyan Zhong[1,*], Jian Liu[2,*], Yan Luo[1], Mei Wu[1], Feng Qiu[1], Hongqing Zhao[1], Yang Liu[1], Yajing Wang[3], Hongping Long[2], Lei Zhao[4], Yuhong Wang[1], Yuanshan Han[2], Pan Meng[1]

[1]Science & Technology Innovation Center, Hunan University of Chinese Medicine, Changsha, Hunan, 410208, People's Republic of China; [2]The First Hospital, Hunan University of Chinese Medicine, Changsha, Hunan, 410007, People's Republic of China; [3]Office of Science & Technology, Hunan University of Chinese Medicine, Changsha, Hunan, 410208, People's Republic of China; [4]School of Integrated Chinese and Western Medicine, Hunan University of Chinese Medicine, Changsha, Hunan, 410208, People's Republic of China

*These authors contributed equally to this work

Correspondence: Yuanshan Han, The First Hospital, Hunan University of Chinese Medicine, Changsha, Hunan, 410007, People's Republic of China, Email 121983755@qq.com; Pan Meng, Science & Technology Innovation Center, Hunan University of Chinese Medicine, Changsha, Hunan, 410208, People's Republic of China, Email 004181@hnucm.edu.cn

Background: Depression, a leading cause of disability worldwide, is characterized by dysfunction of immature neurons, resulting in dysregulated calcium homeostasis and impaired structural plasticity. Jujuboside A (JuA), a biologically active compound derived from *Semen Ziziphi Spinosae*, has demonstrated anti-anxiety and anti-insomnia properties. Recent studies suggest that JuA may be a promising antidepressant, but its underlying mechanisms remain unclear.

Methods: Sprague-Dawley rats were subjected to chronic unpredictable mild stress (CUMS) to induce a depression model. JuA (12.5 mg/kg, 25 mg/kg, 50 mg/kg) was administered orally for 4 weeks. Emotional and cognitive function were assessed. Monoamine neurotransmitter levels were measured using enzyme-linked immunosorbent assay (ELISA). The number of immature neurons and calcium homeostasis were evaluated by immunofluorescence. Western blotting and immunofluorescence were employed to detect the expression of Sonic hedgehog (Shh) signaling proteins. Additionally, lentiviral vector expressing Shh shRNA (LV-Shh-RNAi) were infused intracerebrally to investigate the role of Shh in JuA's antidepressant effects.

Results: JuA significantly ameliorated depressive-like behavior and cognitive dysfunction in CUMS rats, increased monoamine neurotransmitter levels in serum and hippocampal tissue, reduced the number of BrdU/DCX (bromodeoxyuridine/doublecortin)-positive immature neurons, and attenuated calcium ion (Ca^{2+}) concentration and Ca^{2+}/calmodulin-dependent protein kinase II (CaMKII) levels in immature neurons. JuA also markedly elevated synaptic density and prominence complexity, upregulated Shh, Gli family zinc finger 1 and 2 (Gli1/2), synaptophysin (Syn) and postsynaptic density protein-95 (PSD-95) expression in the ventral dentate gyrus (vDG). However, knockdown of Shh in the vDG counteracted JuA's therapeutic effects.

Conclusion: These findings collectively suggest that JuA improves depressive-like behavior in CUMS rats by modulating calcium homeostasis and synaptic structural plasticity in immature neurons through the Shh signaling pathway.

Keywords: Jujuboside A, Sonic hedgehog, Immature neuron, Calcium homeostasis, Depression

Introduction

Depression is one of the leading causes of disease burden worldwide, which is expected to be a major cause of disability by 2030.[1] Despite the progress made in recent years in exploring the molecular and subcellular levels of depression, the pathogenesis of the disease remains unclear.[2] Hippocampal neuronal abnormalities are reportedly closely associated with the development of depression. While most research has concentrated on mature hippocampal neurons, accumulating evidence suggests that immature neurons, characterized by higher excitability, plasticity, and distinct neurotransmission profiles, may play a potential role in depression.[3] It has been shown that chronic stress can lead to the development of

Received: 7 July 2024
Accepted: 20 September 2024
Published: 12 October 2024

depressive-like behaviors by reducing the number and altering the morphology of immature neurons.[4] Notably, the effects of stress on immature neurons were more pronounced in the ventral hippocampus (vHip), suggesting that the immature neurons plays a pivotal role in the formation of vHip functionality, such as emotional regulation.[5] Therefore, investigation of immature neurons within the vHip in depression may offer novel avenues for therapeutic intervention.

Calcium ions (Ca^{2+}) control a wide range of signals for the physiological function of neuronal cells and can transmit depolarization states and synaptic activity to neurons in response to adaptive structural and functional changes in neuronal networks. Restoration of calcium homeostasis attenuates the activation of neuronal destructive pathways and has a favorable neuroprotective potential.[6] Previously, it has been reported that verbascoside can exert antidepressant-like effects by regulating calcium homeostasis.[7] Therefore, regulating calcium homeostasis to improve neuronal dysfunction may be a potential mechanism of action for antidepressants.

Synapses are the fundamental structural units that facilitate neuronal information transmission. A growing body of research supports the critical role of synaptic plasticity in depression.[8] Synaptic structural plasticity is considered to be the physiological basis of synaptic plasticity. Alterations in synapse number, dendritic spine structure, postsynaptic density, and spine morphology can lead to changes in synaptic structural plasticity.[9] There is an increasing consensus suggesting that synaptic structural plasticity is abnormal in patients with depression, and alterations in the morphology of immature neurons can contribute to functional integration disorders. In this respect, studies have reported that prometha-zine ameliorates depressive symptoms by blocking changes in dendritic spine structure in mice.[10] Hence, maintaining synaptic structural plasticity might help generate novel therapeutic targets for antidepressants.

Sonic hedgehog (Shh) is reportedly implicated in neuronal survival and encourages the development of newborn neurons.[11] A study suggested that inhibition of Shh in the ventral dentate gyrus (vDG) resulted in delayed maturation of immature neurons and impaired neuronal activity.[12] Further studies have found that the knockdown of Shh resulted in multiple developmental defects in neurons, indicating that the effective integration of newborn neurons is dependent on Shh signaling.[13] Earlier studies have also reported that Shh modulates hippocampal neuronal circuit formation and adaptive plasticity throughout life by regulating axon growth and synaptogenesis.[14] However, it has not been reported whether Shh can modulate calcium homeostasis and synaptic structural plasticity in immature neurons.

Jujuboside A (JuA), a triterpene saponin isolated from *Semen Ziziphi Spinosae*, has been shown to possess numerous positive effects, including antioxidant, anti-inflammatory, anti-apoptotic, and neuroprotective properties.[15–17] Studies have demonstrated that JuA significantly upregulates the expression of proteins such as brain-derived neurotrophic factor (BDNF), tropomyosin receptor kinase B (TrkB), and cyclic-AMP response binding protein (CREB) in the hippocampus of corticosterone-induced depressed mice. Additionally, JuA markedly enhances the survival of hippocampal neuronal cells (HT22) in vitro.[18] Furthermore, as a neuroprotective agent, JuA has been shown to partially activate the Wnt/β-catenin signaling pathway, thereby promoting proliferation and neuronal differentiation of amyloid precursor protein-overexpressing neural stem cells (APP-NSCs) and enhancing hippocampal neurogenesis.[19] According to the above report, JuA demonstrates good potential antidepressant efficacy. However, whether JuA yields antidepressant effects through Shh signaling remains to be elucidated.

Herein, we investigated the beneficial effects of JuA on calcium homeostasis and synaptic plasticity in immature neuron of rats subjected to chronic unpredictable mild stress (CUMS), which contributing to the elucidation of its mechanisms of action. Notably, our findings provide valuable insights for future research in exploring the antidepressant properties and mechanisms of JuA.

Material and Methods

Experiment Design

This study was divided into the following two parts.

Experiment 1: Rats were randomly divided into six groups (n = 6 rats/group): Control, CUMS, Flu (Fluoxetine), JuA-H, JuA-M, and JuA-L. Except for the control group, all rats underwent a CUMS regimen for 28 days. Flu, a classic antidepressant, served as the positive control.[20] Rats in the Flu group received an oral dose of 10 mg/kg. JuA-H, JuA-M, and JuA-L groups were administered orally at doses of 50 mg/kg, 25 mg/kg, and 12.5 mg/kg, respectively. The experimental procedures are depicted in Figure 1A.

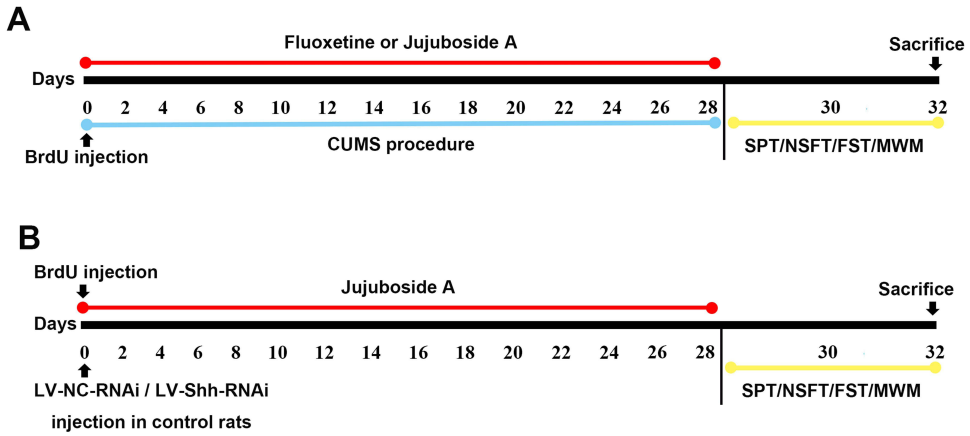

Figure 1 Experiment Design. **(A)** The experimental procedure used to investigate the JuA on depression-like behavior; **(B)** The experimental procedure used to investigate the effect of Shh on the treatment of JuA.

Abbreviations: BrdU, bromodeoxyuridine; CUMS, chronic unpredictable mild stress; SPT, sucrose preference test; NSFT, novelty-suppressed feeding test; FST, forced swimming test; MWM, Morris Water Maze; LV-NC-RNAi/LV-NC, lentiviral vector normal control shRNA; LV-Shh-RNAi/LV-Shh, lentiviral vector expressing Shh shRNA.

Experiment 2: Thirty-six rats were divided into six groups (n = 6 rats/group): (a) Control (non-stressed), (b) CUMS, (c) CUMS treated with JuA at 50 mg/kg (CUMS+JuA), (d) CUMS treated with JuA at 50 mg/kg but subjected to a sham procedure (CUMS+JuA+Sham), (e) CUMS treated with JuA at 50 mg/kg and lentiviral vector normal control shRNA (CUMS+JuA+LV-NC), and (f) CUMS treated with JuA at 50 mg/kg and lentiviral vector expressing Shh shRNA (CUMS +JuA+LV-Shh). The experimental procedures are illustrated in Figure 1B.

Animals

Two batches of eight-week-old male Sprague-Dawley (SD) rats (n = 72), weighing 180–220 g, were obtained from Hunan SJA Laboratory Animal Co., Ltd. The study protocol was approved by the Experimental Animal Ethics Committee of Hunan University of Chinese Medicine (Approval No.: LLBH-202011040002). All animal experiments adhered strictly to the National Institutes of Health Guide for the Care and Use of Laboratory Animals and the Hunan University of Chinese Medicine animal guidelines. All rats were housed in specific pathogen-free (SPF) animal facilities under a temperature-controlled environment (25 ± 1°C) and humidity (50 ± 5%). A 12-hour light-dark cycle was maintained, with food and water available *ad libitum*.

Drugs and Reagents

Fluoxetine hydrochloride capsules (20 mg/capsule; lot number 2019024) were obtained from Lilly Suzhou Pharmaceutical Co., Ltd. Jujuboside A (JuA; MUST-22073110) was acquired from Chengdu Manchester Biotechnology Co., Ltd. Bromodeoxyuridine (BrdU; #B5002) was purchased from Sigma (St. Louis, MO, USA) and dissolved in 0.9% sodium chloride solution. BrdU was administered intraperitoneally at a final dosage of 50 mg/kg, given at 12-hour intervals during the first three days and with six injections.

Chronic Unpredictable Mild Stress Protocol

The sample size for animal experiments was calculated using the Resource Equation Method.[21] Based on the formula n = 10/(k+1) (where k is the number of groups and n is the number of subjects per group), a minimum of three rats per group was determined. To ensure sufficient experimental data, the sample size was increased to six rats per group. Due to variations in sample handling across experiments, a minimum sample size was utilized in some cases. Model rats underwent a 28-day CUMS protocol, consisting of daily exposure to one of seven stressors: (1) 24-hour fasting, (2) 24-hour water deprivation, (3) 24-hour damp bedding, (4) 3-minute electrical shocks, (5) 1-minute tail nip, (6) 3-minute cold water soak (4°C), or (7) 4-hour noise exposure. The same stressor was not repeated within a three-day period.

Stereotaxic Injection of the Lentivirus

Rats were anesthetized, immobilized in a stereotactic brain injector, and underwent aseptic preparation of the cranial region. A small incision was made, and the meninges were removed using a cotton swab soaked in hydrogen peroxide. A skull incision was then made. Lentiviral vector expressing Shh shRNA (LV-Shh-RNAi) (Shanghai GeneChem Corporation, China) was used to inhibit Shh expression in the vDG, and lentiviral vector normal control shRNA (LV-NC-RNAi) served as a control. Coordinates referenced from bregma were used to bilaterally inject 2 μL of lentivirus into the vDG using a microsyringe pump (ZS Dichuang, Beijing, China) at AP: −4.5 mm, ML: ±3.0 mm, and DV: −4.0 mm. Rats were allowed a three-day recovery period post-surgery. Only data from rats with accurately placed injections within the vDG were included in the analyses.

Behavioral Tests

Sucrose Preference Test (SPT)

Rats underwent adaptive training with both pure water and a 1% sucrose solution. Two days prior to testing, each rat was presented with a choice between 50 mL of pure water and 50 mL of 1% sucrose solution. The bottle positions were switched daily to prevent bias from side preferences. The testing period was four hours, with bottle positions alternated every two hours. Sucrose preference was calculated as a percentage using the formula: sucrose preference (%) = sucrose solution consumption (mL)/(sucrose solution consumption (mL) + water consumption (mL)) × 100%.

Novelty-Suppressed Feeding Test (NSFT)

The NSFT measured the latency of rats to ingest food after a 24-hour food deprivation period, while water continued to be provided *ad libitum*. Rats were placed in a black open field box (100×100×20 cm) under bright light, and the time taken to begin chewing a standard food pellet in the center was recorded within 6 minutes. Following the test, rats were returned to their cages, and their food intake was monitored for 6 minutes.

Forced Swimming Test (FST)

Rats were subjected to a forced swimming test in a plexiglass cylinder (height: 45 cm; diameter: 25 cm) filled with water at a temperature of 22–25°C to a depth of 30 cm. The test duration was 6 minutes, with a 2-minute acclimatization period. Immobility, defined as floating effortlessly to keep the head above water, was recorded for the subsequent 4 minutes. Following each trial, rats were dried and returned to their original cages.

Morris Water Maze (MWM)

The rats underwent Morris water maze testing in a circular pool (120 cm height, 40 cm diameter) filled with 22–25°C water to a depth of 30 cm. A hidden platform (28 cm height, 10 cm diameter) was submerged 2 cm below the water surface in one quadrant. Rats received daily 2-minute of platform search training per day. Successful platform location allowed for a 30-second rest, while unsuccessful attempts resulted in gentle guidance to the platform for 30 seconds. On fifth day, the time taken to find the platform within 2 minutes was recorded. On sixth day, the platform was removed, and the time spent in the original platform quadrant within 120 seconds was measured. A data acquisition system (ZS-001, Beijing Zhongshidichuang Company) was used to collect and analyze all data.

Enzyme-Linked Immunosorbent Assay (ELISA)

Following the trial, rats were anesthetized, and whole blood was collected from the abdominal aorta using a vacuum blood collection tube. The blood was gently shaken, mixed thoroughly, and centrifuged at 4°C for 10 minutes at 3000 revolutions per minute after a 30-minute standing period. The upper serum layer was extracted.[22] After euthanasia, the hippocampus of rats were rapidly dissected, and tissue homogenates were prepared according to the kit instructions. ELISA kits for 5-hydroxytryptamine (5-HT, Cat. E-EL-0033c), dopamine (DA, E-EL-0046c), and norepinephrine (NE, Cat. E-EL-0047c) were obtained from Elibscience (Wuhan, China). The manufacturer's guidelines were followed, and absorbance values were measured at the specified wavelengths.

Measurement of Intracellular Calcium Ion Concentration in the Hippocampus

Fura-2/AM, at a final concentration of 5 μL/L, was added to a cell suspension of 10^6 cells/mL, which was then incubated for 45 minutes in a 37°C incubator with 5% CO_2 as previously described.[23] Fluorescence intensity measurements were acquired using a fluorescence microscope with excitation wavelengths ranging from 340 to 380 nm and an emission wavelength of 510 nm. The ratio of fluorescence intensities at 340 nm and 380 nm (R) was calculated. The intracellular Ca^{2+} concentration in the hippocampus was calculated according to the following equation, $[Ca^{2+}]= K_d\ (R-R_{min})/(R_{max}-R_{min})$, where K_d denotes the effective dissociation constant of Fura-2, R_{max} denotes the fluorescence intensity value measured after the addition of Triton X-100, and R_{min} denotes the fluorescence intensity value measured after the addition of EDTA.

Golgi Staining

Fresh brain tissue blocks were subjected to Golgi staining according to the manufacturer's instructions. The morphology and density of pyramidal neurons and dendrites in the vDG of rats were examined using light microscopy. Dendritic spines were counted and measured in length with Image J 6.0 software, and the total density of dendritic spines was calculated.

Western Blotting Analysis

Following the euthanasia of the rats, their brains were promptly removed, and the ventral hippocampal region, specifically located between −5.30 and −6.1 mm from bregma, was identified using a three-dimensional localization coordinate map. The vDG was then carefully isolated under a stereomicroscope at a magnification of 10x.[12] To quantify protein concentrations in the tissue samples, commercial kits were employed according to the manufacturer's protocols. Subsequently, 20 μg of protein from each sample was separated using sodium dodecyl sulfate-polyacrylamide gel electrophoresis (SDS-PAGE) and transferred onto a polyvinylidene fluoride (PVDF) membrane. The membrane was subsequently blocked with 5% skim milk for 1–2 hours. Primary antibodies, including anti-Shh (Proteintech, 20697-1-AP, 1:1000), anti-Gli family zinc finger 1 (Gli1, Zeye, ZY-3098Ab, 1:1500), anti-Gli family zinc finger 2 (Gli2, Proteintech, 18989-1-AP, 1:1000), anti-postsynaptic density protein-95 (PSD-95, Proteintech, 20665-1-AP, 1:5000), anti-synaptophysin (Syn, Proteintech, 17785-1-AP, 1:2000), and anti-β-actin (Servicebio, GB15003, 1:3000) at 4°C overnight. The membranes were then incubated with the corresponding secondary antibody (Eliascience, E-AB-1001, 1:10,000,) at 37°C for 1 hour. After washing, gray-scale values of protein electrophoresis bands were visualized by the ChemiDoc XRS imaging system (Bio-Rad, Hercules, CA, USA).

Immunofluorescence (IF) Staining

After antigen retrieval, the sections were blocked with 3% BSA for 1 hour. Next, the sections were incubated with primary antibodies: mouse-anti-BrdU (CST, #5292, 1:1000) following pretreatment, rabbit-anti-Shh (Proteintech, 20697-1-AP, 1:100), rabbit-anti-Gli1 (Bioss, bs-1206R, 1:500), rabbit-anti-Gli2 (Proteintech, 18989-1-AP, 1:500), goat-anti-doublecortin (DCX, Proteintech, 13925-1-AP, 1:100), rabbit-anti-Ca^{2+}/calmodulin (CaM)-dependent protein kinase II (CaMKII, Abcam, ab134041, 1:300), rabbit-anti-C-fos proto-oncogene protein (C-fos, Affinity, AF0132, 1:100), anti-PSD-95 (Proteintech, 20665-1-AP, 1:100) and rabbit-anti-Syn (Proteintech, 67864-1-lg, 1:100) at 4°C overnight. After washing with PBS, the sections were treated with the corresponding secondary antibodies (goat anti-rabbit 594 [Abcam, ab150080, 1:600] and donkey anti-goat 488 [Abcam, ab150129, 1:800]) at room temperature for 1 hour, followed by another PBS rinse. Panoramic MIDI (Servicebio) was used to capture tissue immunofluorescence images. Image J software was then used to quantify the number of positive cells.

Statistical Analysis

All collected data were analyzed with IBM SPSS Statistics 25.0 software. Data were presented as mean ± SD. Each experiment for each group was independently repeated at least three times. To assess the normality of data distribution, the Shapiro–Wilk test was applied, and all data passed the normality test. Two-way ANOVA with Bonferroni correction

or one-way ANOVA with Tukey's post-hoc test was employed for statistical analysis. For datasets with a sample size of n=3, data were analyzed using the permutation test. A *p-value* of less than 0.05 ($p < 0.05$) was considered statistically significant.

Results

JuA exerted an antidepressant effect by ameliorating depression-like behavior and monoamine neurotransmitter levels

Following four weeks of CUMS modeling, the effect of JuA on depression was investigated by behavioral tests. To determine the optimal dose of JuA, doses of 12.5, 25, and 50 mg/kg were administered, and behavioral impairment was evaluated using SPT, NSFT, FST, and MWM tests. In our results, rats exposed to CUMS exhibited a significant reduction in sucrose consumption percentage in the SPT compared to controls (Figure 2A; $p < 0.01$). However, in rats treated with a high dosage of JuA, sucrose consumption increased ($p < 0.01$). Similarly, in the NSFT, CUMS-exposed rats displayed an increased latency to feed compared to controls (Figure 2B; $p < 0.05$). Flu and high dosages of JuA reversed this increase in latency ($p < 0.05$, $p < 0.05$), with no observed changes in home food consumption. Furthermore, CUMS rats exhibited a dramatic increase in immobility time in the FST (Figure 2C; $p < 0.01$), which was significantly improved by treatment with both the high and medium dosages of JuA ($p < 0.01$, $p < 0.01$). In the MWM, CUMS rats displayed an increased escape latency and decreased swimming time in the target quadrant (Figure 2D and E $p < 0.01$ for both), effects reversed by treatment with 50 mg/kg JuA ($p < 0.01$ for both). In addition, our investigation explored the impact of JuA on monoamine neurotransmitter levels of serum and hippocampus, as depicted in Figure 2F and G. In comparison to the control group, CUMS rats exhibited a significant reduction in the serum and hippocampal levels of 5-HT, DA, and NE ($p_s < 0.01$). Conversely, 50 mg/kg JuA effectively restored the attenuated levels of 5-HT, DA, and NE in both serum and hippocampus ($p_s < 0.01$).

JuA Countered CUMS-Induced Inhibition of Shh Signaling and Deficits in Immature Neurons Within vHip

To evaluate the effects of JuA on immature neurons of the vHip, the co-expression of BrdU with DCX was investigated (Figure 3A and C). JuA treatment improved the number of BrdU/DCX-positive immature neurons in the vDG compared with the CUMS group ($p < 0.05$). This confirmed that JuA's effects in promoting neural stem cell (NSC) differentiation may contribute to the increase in DCX-positive cells. Immunofluorescence results revealed that the expression levels of Shh, Gli1, and Gli2 in the vDG were markedly higher in the JuA treatment (50 mg/kg) group than that in the CUMS group ($p < 0.05$ for all; Figure 3B and D). Western blotting supported these findings, demonstrating that JuA treatment increased Shh expression in the vDG, especially at the 50 mg/kg dose ($p < 0.05$; Figure 3E and F). JuA also promoted the levels of Gli1 and Gli2 ($p < 0.05$, $p < 0.05$; Figure 3E and F), proteins associated with Shh signaling. Notably, JuA treatment at 12.5 mg/kg did not induce these changes ($p > 0.05$; Figure 3E and F).

JuA Reversed CUMS-Induced Dysregulation of Calcium Homeostasis in Immature Neurons

Immunofluorescence double staining of immature neurons (DCX-positive) and calmodulin (CaMKII-positive) was used to further elucidate whether JuA protects immature neurons by regulating calcium homeostasis. As shown in Figure 4A and B, compared with the control group, the number of $DCX^+/CaMKII^+$ cells was significantly elevated in CUMS rats ($p < 0.05$). JuA-H treatment dramatically reduced the number of $DCX^+/CaMKII^+$ cells in immature neurons ($p < 0.05$; Figure 4A and B), while JuA-M and JuA-L tended to reduce the number of $DCX^+/CaMKII^+$ cells, although the difference was not statistically significant ($p > 0.05$). In addition, the Ca^{2+} concentration assay showed that JuA significantly reversed the CUMS-induced elevation in vHip ($p < 0.05$; Figure 4C).

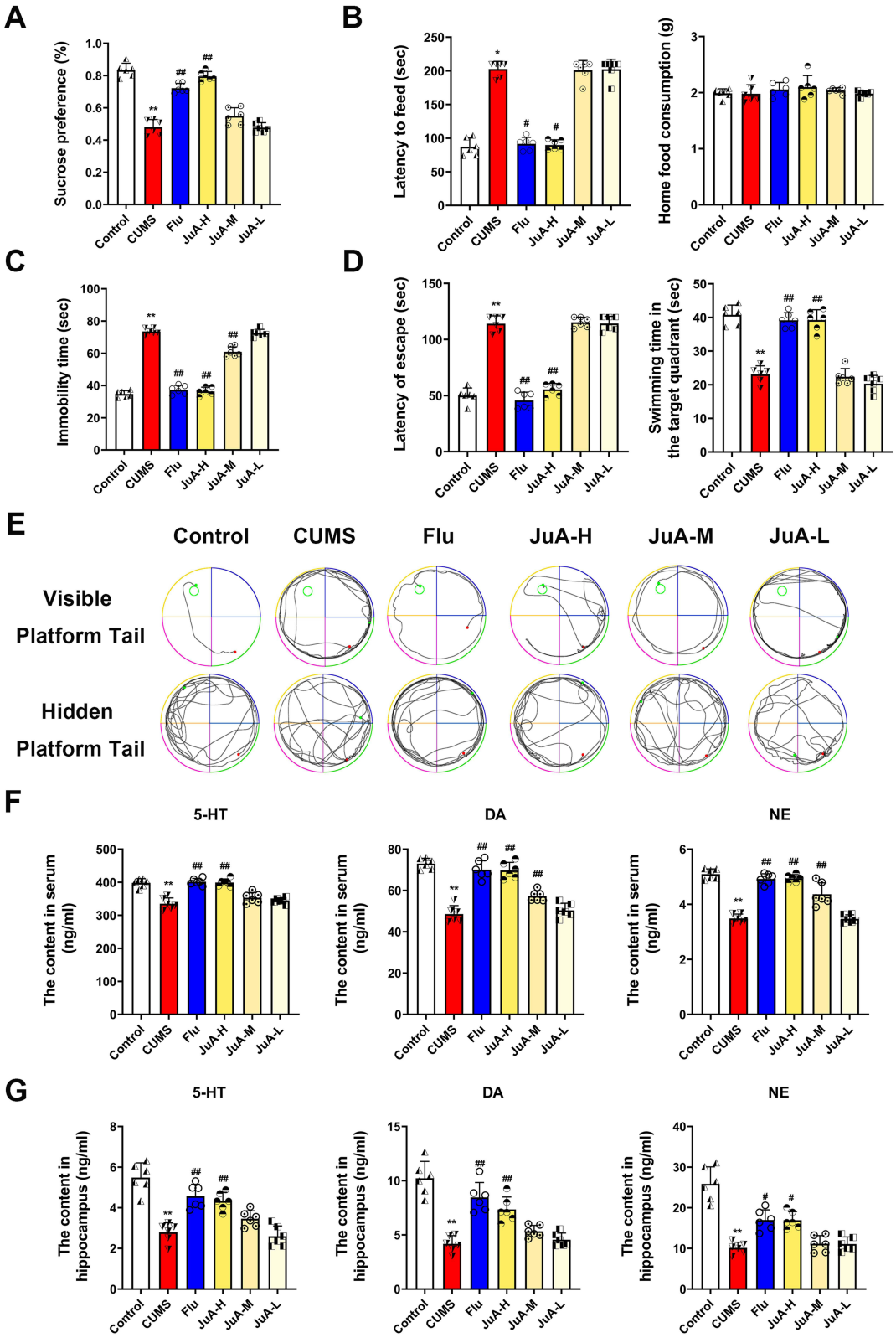

Figure 2 JuA exerts antidepressant-like effects in CUMS-induced depression rat model. **(A)** The sucrose preference in the SPT; **(B)** Latency to feed in the NSFT; Total food consumption in the home-cage in the NSFT. **(C)** Immobility time in the FST; **(D)** Latency of escape in the MWM; Swimming time in the target quadrant in the MWM; **(E)** Trace plot in the MWM. **(F)** Serum levels of 5-HT, DA, NE in rats. **(G)** Hippocampus levels of 5-HT, DA, and NE in rats. n = 6 in each group; the data are presented as the mean ± SD. $^{*}p < 0.05$, $^{**}p < 0.01$ vs. the control group. $^{\#}p < 0.05$, $^{\#\#}p < 0.01$ vs. the CUMS group.

Abbreviations: CUMS, chronic unpredictable mild stress; Flu, Fluoxetine; JuA-H, Jujuboside A high-dose (50mg/kg); JuA-M, Jujuboside A medium-dose (25 mg/kg); JuA-L, Jujuboside A low-dose (12.5 mg/kg); 5-HT, 5-hydroxytryptamine; DA, dopamine; NE, norepinephrine.

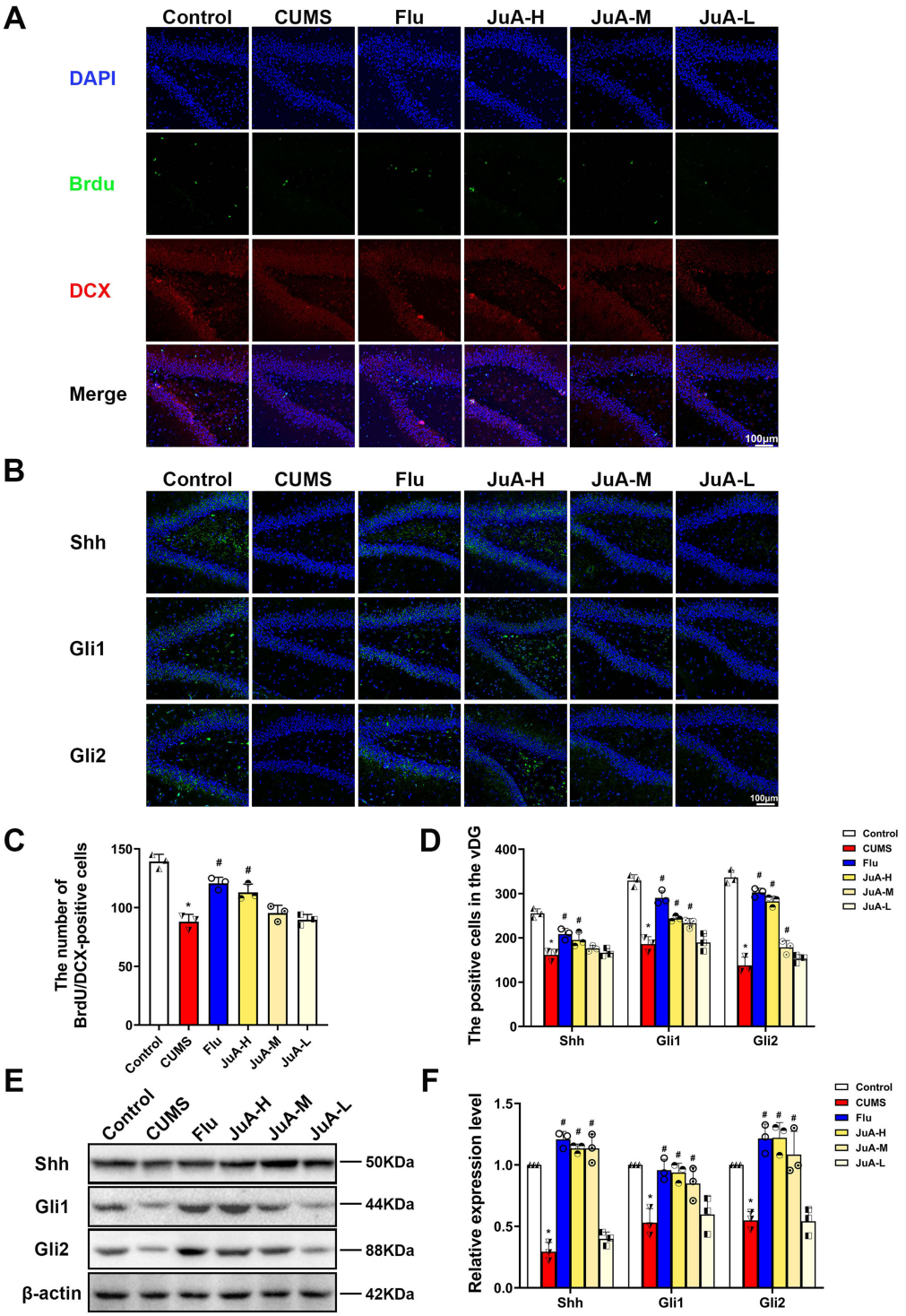

Figure 3 JuA increases the number of immature neurons and activates Shh signaling in the CUMS rats. **(A)** Representative fluorescence images of $BrdU^+/DCX^+$ cells; **(B)** Representative fluorescence images of Shh^+, $Gli1^+$ and $Gli2^+$ cells; **(C)** Number of $BrdU^+/DCX^+$ cells; **(D)** Number of Shh^+, $Gli1^+$ and $Gli2^+$ cells; **(E)** Representative immunoblotting bands of Shh, Gli1, Gli2 in each group; **(F)** Expression levels of Shh, Gli1 and Gli2. n = 3 in each group; the data are presented as the mean ± SD. $^*p < 0.05$ vs the control group. $^{\#}p < 0.05$ vs the CUMS group.

Abbreviations: CUMS, chronic unpredictable mild stress; Flu, Fluoxetine; JuA-H, Jujuboside A high-dose (50mg/kg); JuA-M, Jujuboside A medium-dose (25 mg/kg); JuA-L, Jujuboside A low-dose (12.5 mg/kg); vDG, ventral dentate gyrus; DAPI, 4',6-diamidino-2-phenylindole; BrdU, bromodeoxyuridine; DCX, doublecortin; Shh, sonic hedgehog; Gli1, Gli family zinc finger 1; Gli2, Gli family zinc finger 2.

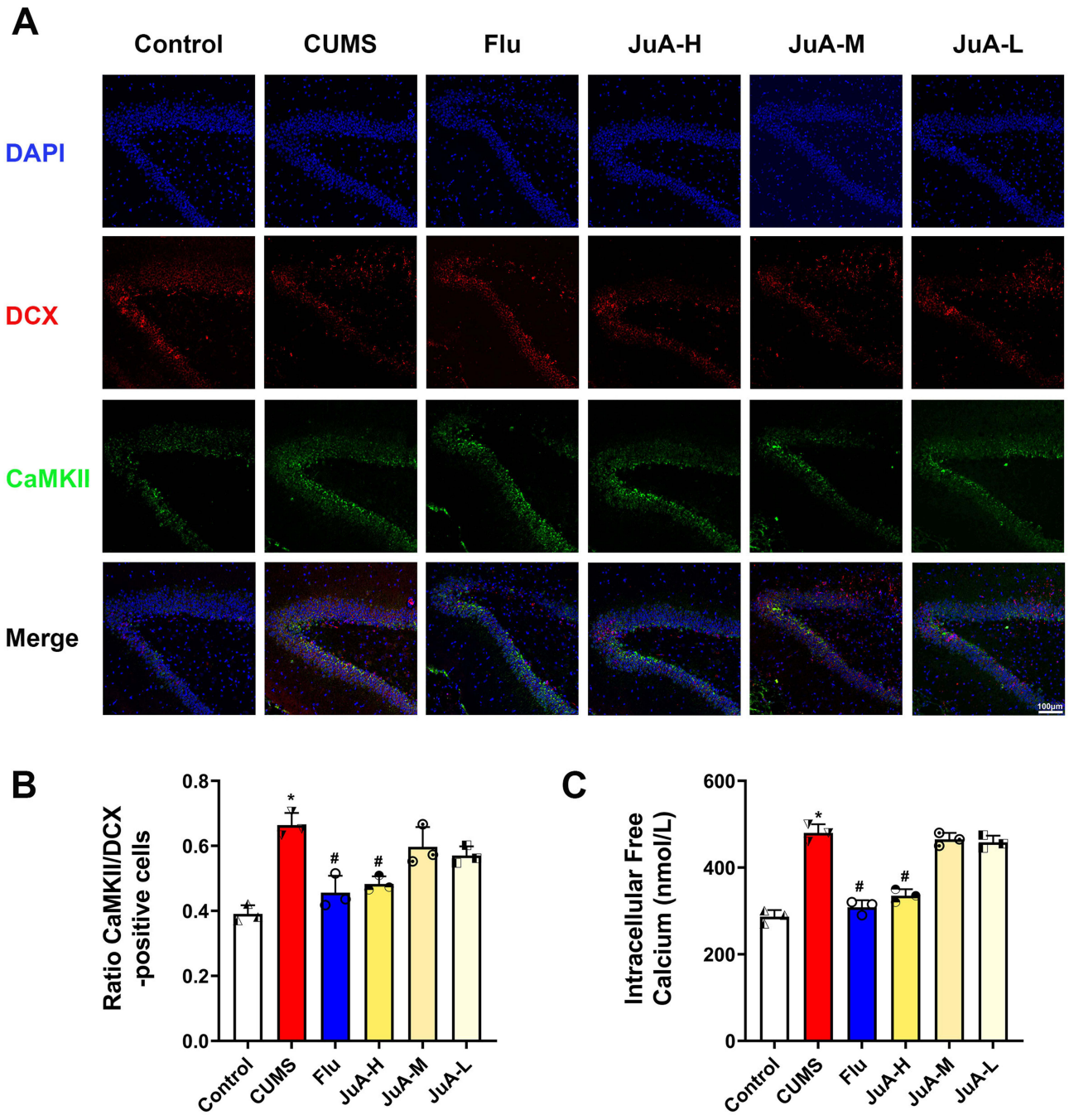

Figure 4 JuA improves dysregulated calcium homeostasis in immature neurons in the vHip. **(A)** Representative fluorescence images of calcium homeostasis in immature neurons; **(B)** The ratio of CaMKII/DCX-positive cells in the vDG; **(C)** Intracellular calcium concentration in the vHip. n = 3 in each group; the data are presented as the mean ± SD. $^{*}p < 0.05$ vs control group. $^{\#}p < 0.05$ vs CUMS group.

Abbreviations: CUMS, chronic unpredictable mild stress; Flu, Fluoxetine; JuA-H, Jujuboside A high-dose (50mg/kg); JuA-M, Jujuboside A medium-dose (25 mg/kg); JuA-L, Jujuboside A low-dose (12.5 mg/kg); DAPI, 4',6-diamidino-2-phenylindole; DCX, doublecortin; CaMKII, the Ca^{2+}/calmodulin (CaM)-dependent protein kinase II.

Knockdown of Shh Eliminated the Antidepressant Effect of JuA

The above results revealed that JuA at a dosage of 50 mg/kg exhibited notable antidepressant properties and appreciably elevated the expression of Shh and its downstream signaling molecules Gli1 and Gli2. To further validate whether JuA exerts its antidepressant effects via Shh signaling pathway, a lentiviral vector engineered to express Shh shRNA (LV-Shh-RNAi) was constructed and bilaterally injected into the vDG to effectively knockdown Shh. Subsequent to the LV-Shh-RNAi injection, rats underwent CUMS modeling and received a 50 mg/kg dose of JuA, followed by behavioral testing

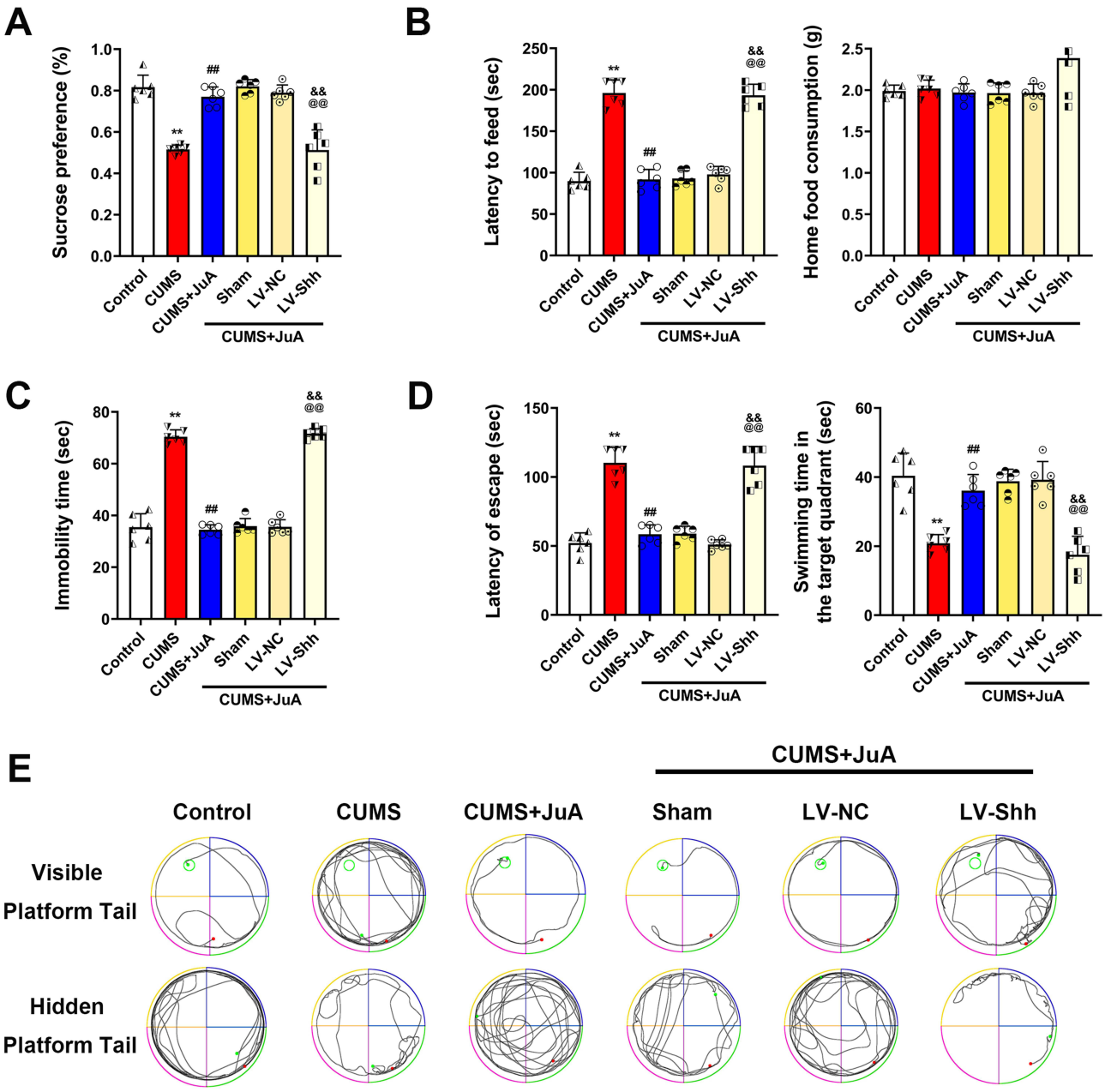

Figure 5 Knockdown of Shh in the vDG eliminates the antidepressant effect of JuA. **(A)** The sucrose preference in the SPT; **(B)** Latency to feed in the NSFT; Total food consumption in the home cage in the NSFT. **(C)** Immobility time in the FST; **(D)** Latency of escape in the MWM; Swimming time in the target quadrant in the MWM. **(E)** Trace plot in the MWM. n = 6 in each group; the data are presented as the mean ± SD. $^{**}p < 0.01$ vs the Control group. $^{\#\#}p < 0.01$ vs the CUMS group. $^{@@}p < 0.01$ vs the LV-NC group. $^{\&\&}p < 0.01$ vs the CUMS+JuA group.

Abbreviations: LV-NC-RNAi/LV-NC, lentiviral vector normal control shRNA; LV-Shh-RNAi/LV-Shh, lentiviral vector expressing Shh shRNA; CUMS, chronic unpredictable mild stress; CUMS+JuA, CUMS treated with JuA at 50 mg/kg; CUMS+JuA+Sham, CUMS treated with JuA at 50 mg/kg but subjected to a sham procedure.

(Figure 1B). The results showed that knockdown of Shh significantly decreased sucrose consumption ($p < 0.01$) and swimming time in the target quadrant ($p < 0.01$), while increasing latency to feed ($p < 0.01$), immobility times ($p < 0.01$), and latency of escape ($p < 0.01$; Figure 5), compared to the CUMS + JuA group.

Knockdown of Shh Altered the Effect of JuA on Shh Signaling

To verify the specificity and efficacy of knocking down Shh in *vivo*, we analyzed the level of Shh in the vDG and found that Shh expression was significantly suppressed in the LV-Shh-RNAi group ($p < 0.05$; Figure 6A and B). Importantly,

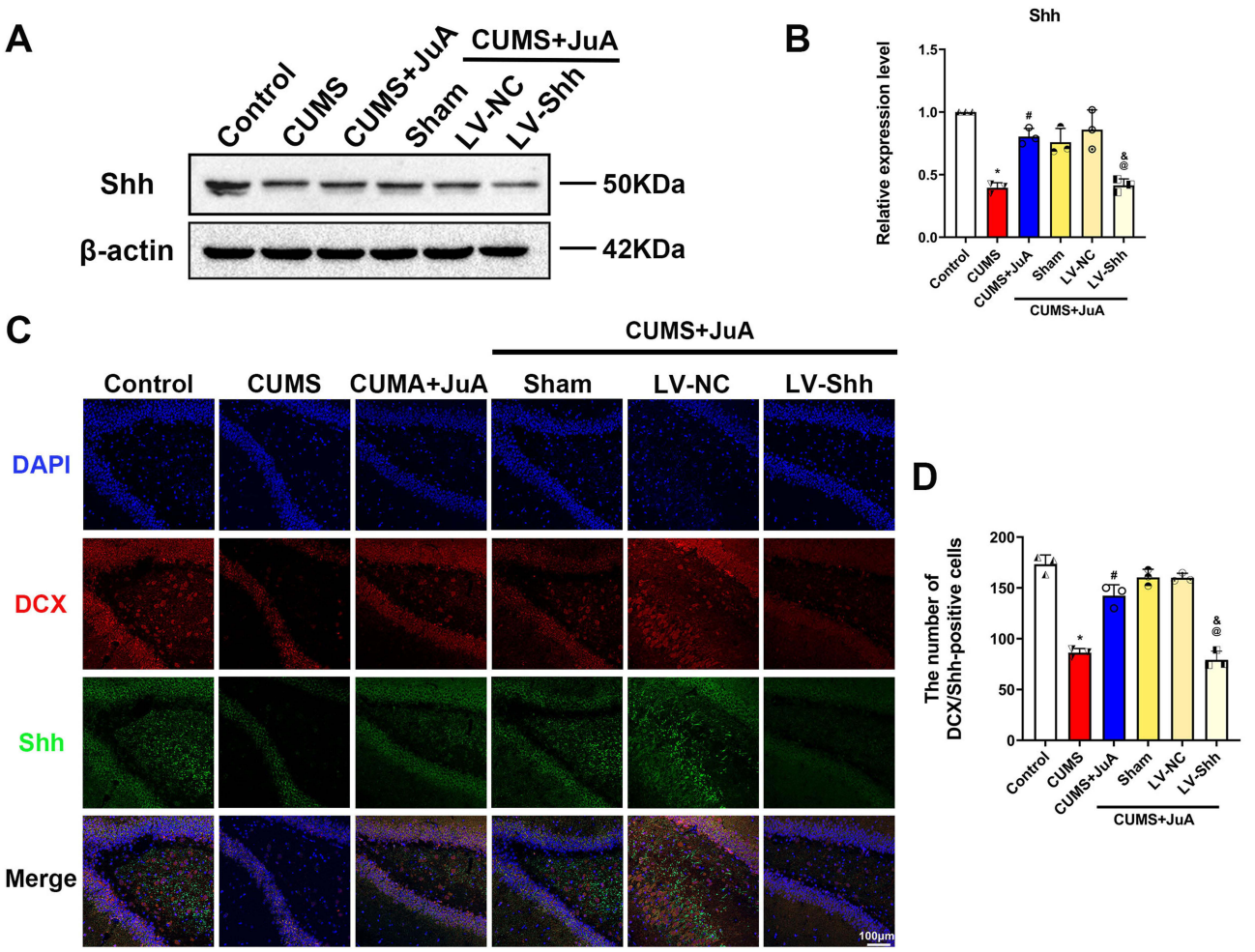

Figure 6 Knockdown of Shh counters the therapeutic effect of JuA on Shh signaling in vDG. **(A)** Representative immunoblotting bands of Shh in each group; **(B)** Expression levels of Shh in the vDG; **(C)** Representative fluorescence images of DCX^+/Shh^+ cells in rats; **(D)** Number of DCX^+/Shh^+ cells in the vDG; n = 3 in each group; the data are presented as the mean ± SD. $^*p < 0.05$ vs the Control group. $^{\#}p < 0.05$ vs the CUMS group. $^{@}p < 0.05$ vs the LV-NC group. $^{\&}p < 0.05$ vs the CUMS+JuA group.
Abbreviations: CUMS, chronic unpredictable mild stress; CUMS+JuA, CUMS treated with JuA at 50 mg/kg; CUMS+JuA+Sham, CUMS treated with JuA at 50 mg/kg but subjected to a sham procedure; LV-NC-RNAi/LV-NC, lentiviral vector normal control shRNA; LV-Shh-RNAi/LV-Shh, lentiviral vector expressing Shh shRNA; Shh, sonic hedgehog; DAPI, 4',6-diamidino-2-phenylindole; DCX, doublecortin.

JuA treatment did not reverse the decrease in Shh signaling observed in the CUMS +LV-Shh-RNAi rats ($p < 0.05$). Next, we examined the abundance of double-positive cells expressing both DCX (immature neuron marker) and Shh in the vDG. As shown in Figure 6C and D, LV-Shh-RNAi treatment notably decreased the number of Shh-positive cells in immature neurons ($p < 0.05$). Interestingly, we observed that LV-Shh-RNAi injection significantly countered the therapeutic effect of JuA ($p < 0.05$).

Knockdown of Shh Impeded the Protective Effect of JuA on Calcium Homeostasis and Neuronal Activation

Immunofluorescence assay results showed that Shh inhibition in the vDG by LV-Shh-RNAi markedly increased the number of $DCX^+/CaMKII^+$ cells ($p < 0.05$; Figure 7A and B). As shown in Figure 7C, LV-Shh-RNAi counteracted the regulatory effect of JuA on Ca^{2+} concentration. In addition, calcium homeostasis is closely related to neuronal activation, and calcium homeostasis can modulate neuronal activation by affecting cell membrane polarization.[24] We investigated whether Shh inhibition affected the activity of immature neurons by quantitatively examining the number of DCX/C-fos-positive cells. The results confirmed that administration of JuA increased the number of DCX/C-fos-positive cells in the

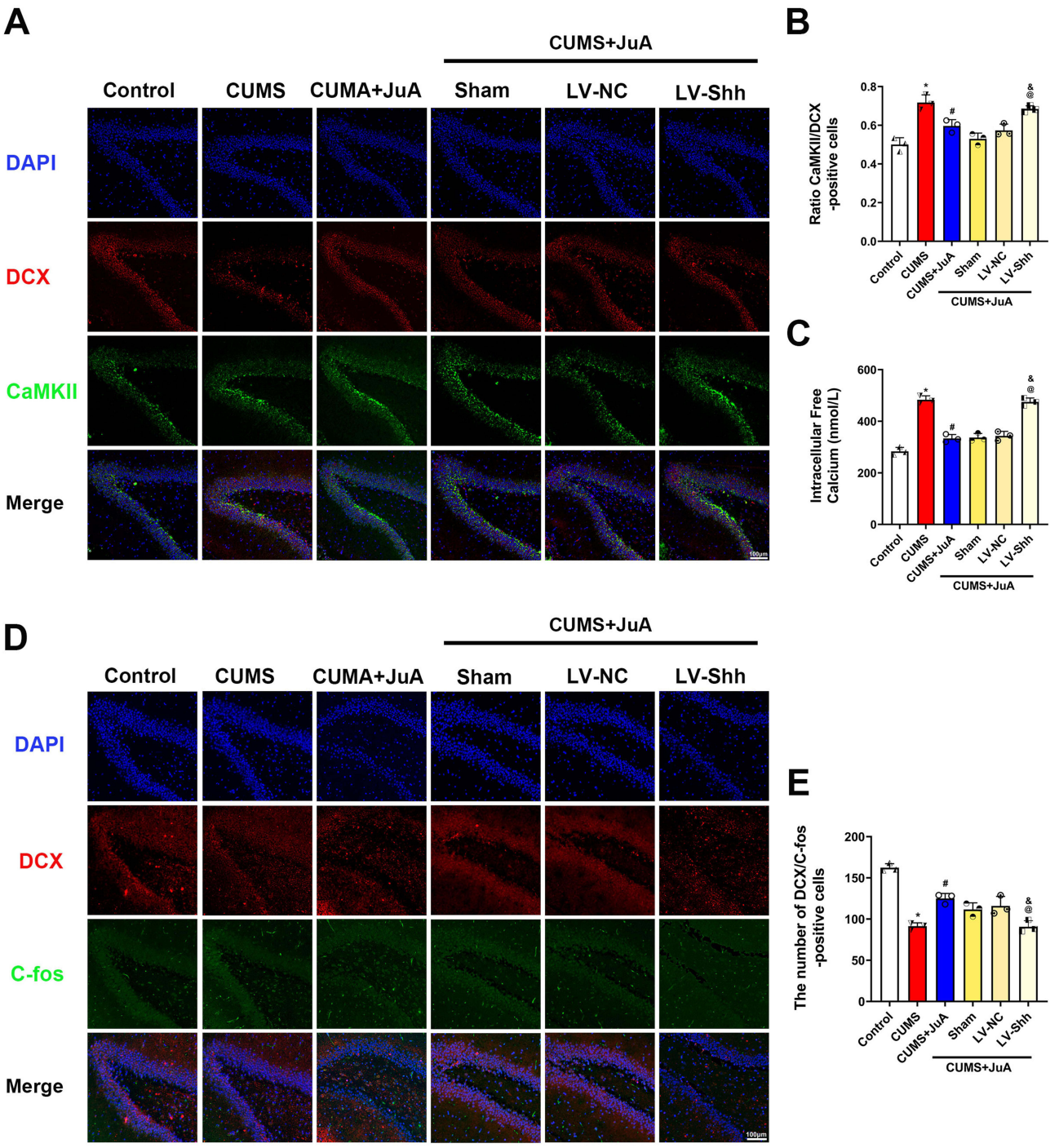

Figure 7 Knockdown of Shh counters the therapeutic effect of JuA on calcium homeostasis in vDG. **(A)** Representative fluorescence images of calcium homeostasis in immature neurons; **(B)** The ratio of CaMKII/DCX-positive cells in the vDG; **(C)** Intracellular calcium concentration in the vHip; **(D)** Representative fluorescence images of $DCX^+/C\text{-}fos^+$ cells in rats; **(E)** Number of $DCX^+/C\text{-}fos^+$ cells in the vDG. n=3 in each group; the data are presented as the mean ± SD. $^*p < 0.05$ vs the Control group. $^{\#}p < 0.05$ vs the CUMS group. $^{@}p < 0.05$ vs the LV-NC group. $^{\&}p < 0.05$ vs the CUMS+JuA group.

Abbreviations: CUMS, chronic unpredictable mild stress; CUMS+JuA, CUMS treated with JuA at 50 mg/kg; CUMS+JuA+Sham, CUMS treated with JuA at 50 mg/kg but subjected to a sham procedure; LV-NC-RNAi/LV-NC, lentiviral vector normal control shRNA; LV-Shh-RNAi/LV-Shh, lentiviral vector expressing Shh shRNA; DAPI, 4',6-diamidino-2-phenylindole; DCX, doublecortin; CaMKII, the Ca^{2+}/calmodulin (CaM)-dependent protein kinase II; C-fos, c-fos proto-oncogene protein.

vDG of CUMS rats ($p < 0.05$), indicating that JuA can enhance the activation of immature neurons. However, LV-Shh-RNAi led to a significantly lower number of DCX/C-fos- positive cells in the vDG compared to the CUMS+JuA group ($p < 0.05$; Figure 7D and E).

Knockdown of Shh Mitigated the Improvement Effect of JuA on Synaptic Structural Plasticity

Activated neurons are now understood to continuously replenish synaptic vesicles to maintain normal synaptic function and structure.[25] To further assess the impact of Shh knockdown on synaptic structural plasticity of immature neurons in the vDG, Golgi staining was used to observe the density, length, and complexity of dendritic spines in the vDG of rats. The results showed that the density, maximum length, total length, and number of intersections of dendritic spines were significantly decreased in CUMS rats ($p_s < 0.05$). Treatment with JuA significantly increased the density, maximum length, total length, and number of intersections of dendritic spines in the vDG of CUMS rats ($p_s < 0.05$; Figure 8A–E), while the effect diminished after administration of LV-Shh-RNAi. Furthermore, we examined protein levels at the synaptic interface using immunofluorescence. Specifically, we studied Syn and PSD-95. JuA treatment significantly increased the double-positive cells for DCX/Syn and DCX/PSD-95 ($p < 0.05$ for both). Conversely, LV-Shh-RNAi significantly reduced the number of DCX^+/Syn^+ and $DCX^+/PSD\text{-}95^+$ cells compared to the CUMS+JuA group ($p < 0.05$ for both; Figure 9A-D). Consistent with this, Western blotting results revealed that inhibition of Shh significantly decreased the expression of Syn and PSD-95 in the vDG of JuA-treated rats ($p < 0.05$ for both; Figure 9E–G).

Knockdown of Shh Counteracted the Regulatory Effect of JuA on Gli1 and Gli2

We further elucidated the expression of Gli1 and Gli2 in immature neurons to investigate whether Shh downstream signaling was involved in the antidepressant effects of JuA. Immunofluorescence showed that the number of $DCX^+/Gli1^+$ and $DCX^+/Gli2^+$ cells in the LV-Shh-RNAi group was significantly reduced compared to the CUMS+JuA group ($p < 0.05$ for both; Figure 10A–D). Then, the levels of Gli1 and Gli2 were examined by Western blotting. Knockdown of Shh significantly decreased the expression of Gli1 and Gli2 in the vDG compared to the JuA treatment ($p < 0.05$ for both; Figure 10E–G).

Discussion

Depression is a mood disorder with high morbidity, mortality, and disability rates, posing a significant threat to human health.[26] While JuA's neuroprotective and antidepressant effects have been documented, the underlying mechanisms remain unclear. This study aimed to identify the mechanisms by which JuA exerts its neuroprotective and antidepressant effects. Mechanistically, JuA improved CUMS-induced depressive-like behavior by ameliorating the calcium homeostasis, neuronal activation, and synaptic structural plasticity of the immature neurons. Furthermore, the study showed that JuA exerted these effects mainly through activating the Shh signaling pathway, and the study further confirmed the direct target of JuA and the detailed mechanism of JuA by in *vivo* injection of LV-Shh-RNAi virus. These findings collectively contribute to a deeper comprehension of the underlying mechanisms governing JuA's antidepressant properties, thereby providing a robust preclinical justification for its potential therapeutic utility in the treatment of depression.

Depression is a complex mood disorder characterized by persistent feelings of sadness, hopelessness, and lack of interest in activities. It is often accompanied by cognitive deficits, such as difficulties with concentration, memory, and decision-making.[27] Behavioral tests like SPT, FST, and NSFT are standard procedures for assessing depression-like behaviors in animal models.[28] The SPT measures anhedonia, a core symptom of depression, with reduced intake indicating decreased reward motivation.[29] The NSFT assesses stress coping mechanisms by measuring the latency to feed in a novel environment; faster feeding indicates a better ability to adapt to challenges, a behavior inversely related to depression.[30] In the FST, increased immobility time reflects a state of despair, another hallmark of depression.[31] Consistent with previous research,[32] our results showed that CUMS rats exhibited reduced sucrose consumption, increased feeding latency, and immobility time.[33] In addition, a study reported that the MWM assessed cognitive function related to adult hippocampal neurogenesis.[34] Consistent with the literature, our results showed that CUMS rats exhibited significantly increased avoidance latency, which JuA treatment effectively reversed. JuA administration significantly ameliorated the depressive-like behaviors observed in CUMS rats, supporting its antidepressant activity as seen in a prior study.[18] Moreover, JuA was observed to concurrently modulate the levels of monoamine neurotransmitters, the primary targets of contemporary antidepressant medications,[35] further providing a rationale for JuA's antidepressant effects.

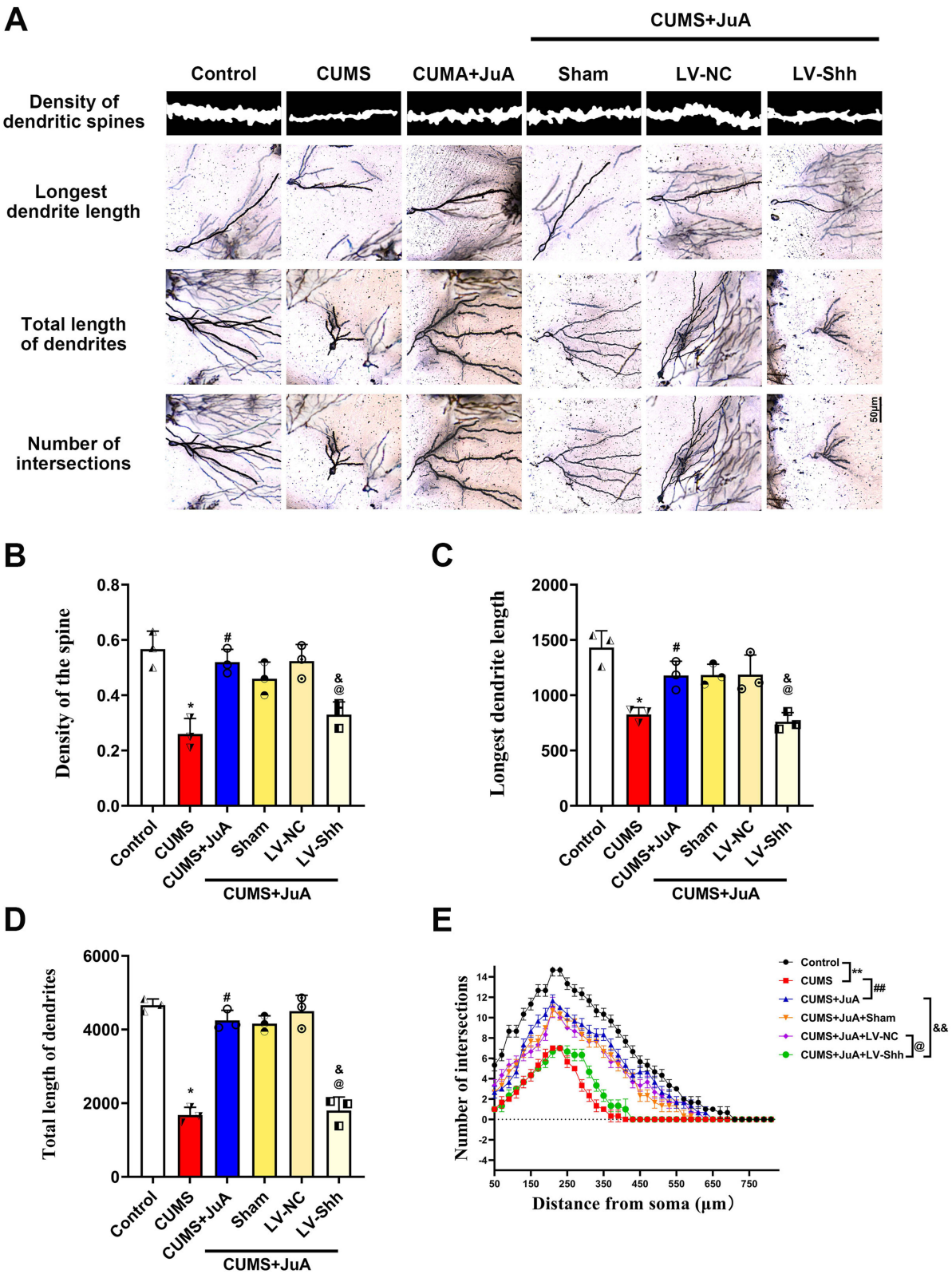

Figure 8 The morphological changes of synapses in vDG by Golgi staining. **(A)** Representative graphs of synapses in the vDG neurons stained by Golgi (200×); **(B)** The density of dendritic spines in each group; **(C)** The longest dendrite length in each group; **(D)** The total length of dendrites in each group; **(E)** The number of dendritic intersections in each group. n=3 in each group; the data are presented as the mean ± SD. $^{*}p < 0.05$, $^{**}p < 0.01$ vs the Control group. $^{\#}p < 0.05$, $^{\#\#}p < 0.01$ vs the CUMS group. $^{@}p < 0.05$ vs the LV-NC group. $^{\&}p < 0.05$, $^{\&\&}p < 0.01$ vs the CUMS+JuA group.

Abbreviations: CUMS, chronic unpredictable mild stress; CUMS+JuA, CUMS treated with JuA at 50 mg/kg; CUMS+JuA+Sham, CUMS treated with JuA at 50 mg/kg but subjected to a sham procedure; LV-NC-RNAi/LV-NC, lentiviral vector normal control shRNA; LV-Shh-RNAi/LV-Shh, lentiviral vector expressing Shh shRNA.

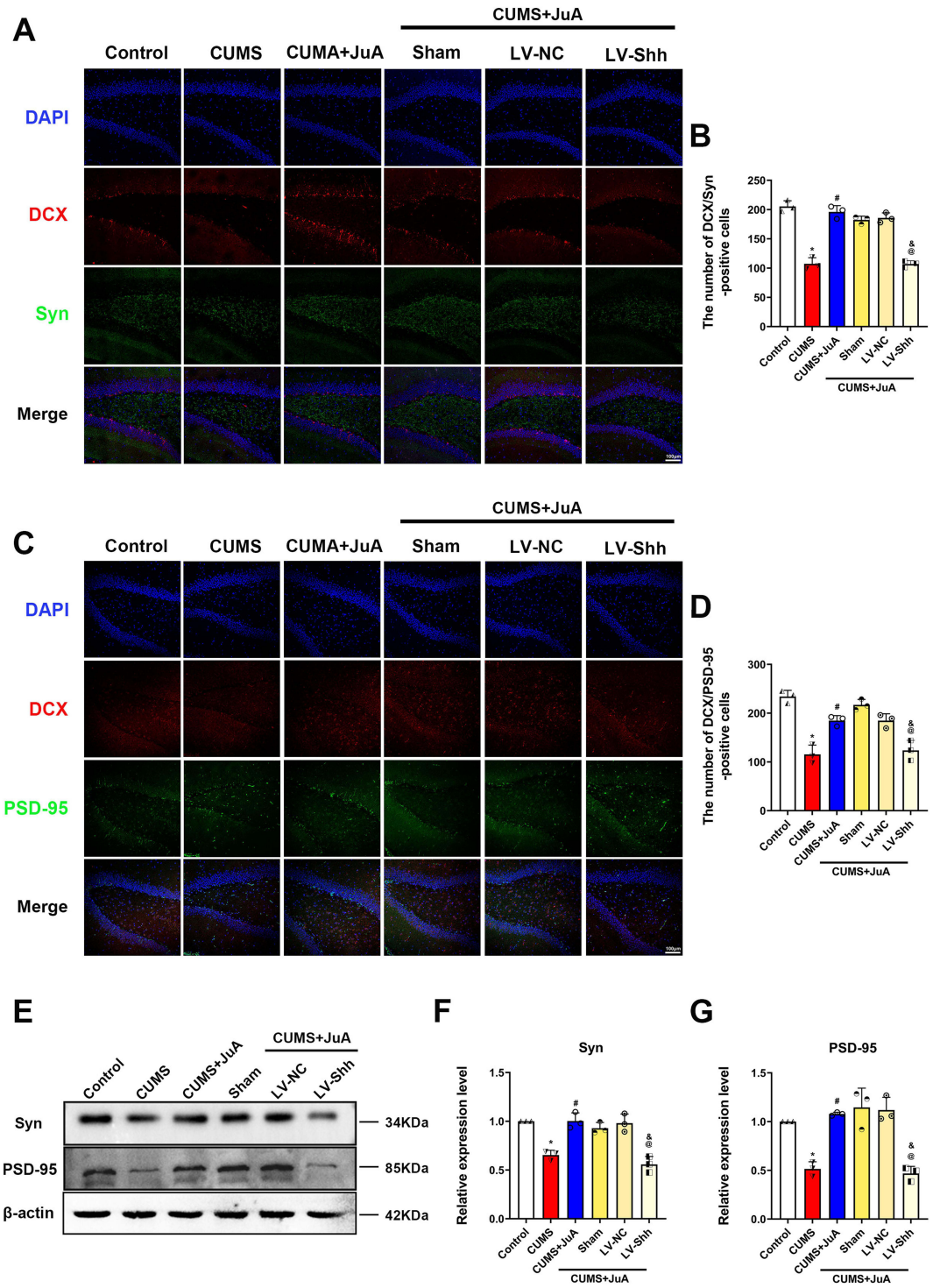

Figure 9 Knockdown of Shh mitigates the improvement of synaptic structural plasticity induced by JuA in immature neurons of vHip. **(A)** Representative fluorescence images of DCX^+/Syn^+ cells in rats; **(B)** Number of DCX^+/Syn^+ cells in the vDG; **(C)** Representative fluorescence images of and $DCX^+/PSD\text{-}95^+$ cells in rats; **(D)** Number of $DCX^+/PSD\text{-}95^+$ cells in the vDG; **(E)** Representative immunoblotting bands of Syn and PSD-95 in each group; **(F)** Expression levels of Syn in the vDG; **(G)** Expression levels of PSD-95 in the vDG. n=3 in each group; the data are presented as the mean ± SD. $^*p < 0.05$ vs the Control group. $^{\#}p < 0.05$ vs the CUMS group. $^{@}p < 0.05$ vs the LV-NC group. $^{\&}p < 0.05$ vs the CUMS+JuA group.

Abbreviations: CUMS, chronic unpredictable mild stress; CUMS+JuA, CUMS treated with JuA at 50 mg/kg; CUMS+JuA+Sham, CUMS treated with JuA at 50 mg/kg but subjected to a sham procedure; LV-NC-RNAi/LV-NC, lentiviral vector normal control shRNA; LV-Shh-RNAi/LV-Shh, lentiviral vector expressing Shh shRNA; DAPI, 4',6-diamidino-2-phenylindole; DCX, doublecortin; Syn, synaptophysin; PSD-95, postsynaptic density protein-95.

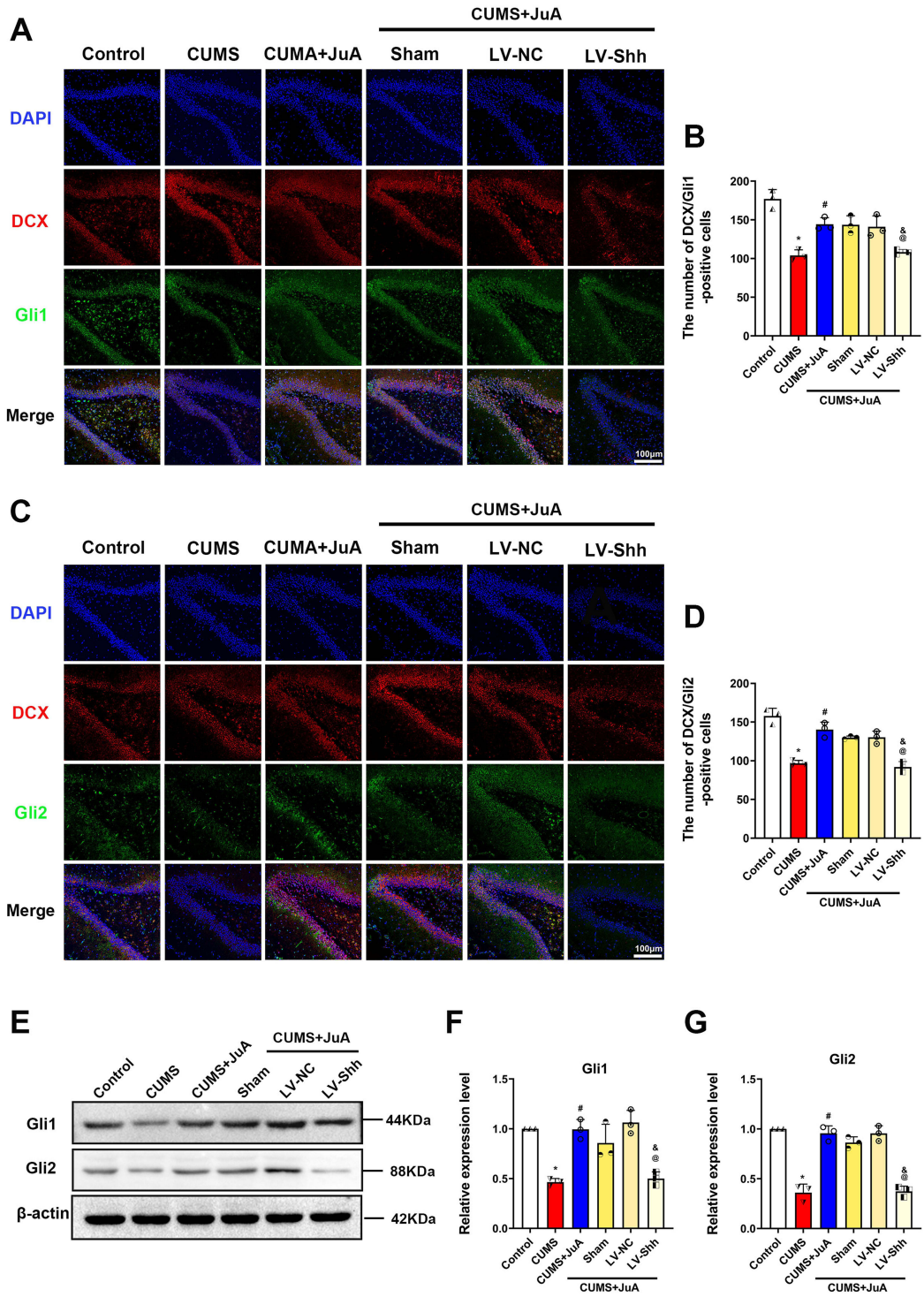

Figure 10 Knockdown of Shh inhibits the activating effect of JuA on the Shh signaling pathway. **(A)** Representative fluorescence images of $DCX^+/Gli1^+$ cells in rats; **(B)** Number of $DCX^+/Gli1^+$ cells in the vDG; **(C)** Representative fluorescence images of and $DCX^+/Gli2^+$ cells in rats; **(D)** Number of $DCX^+/Gli2^+$ cells in the vDG; **(E)** Representative immunoblotting bands of Gli1 and Gli2 in each group; **(F)** Expression levels of Gli1 in the vDG; **(G)** Expression levels of Gli2 in the vDG. n=3 in each group; the data are presented as the mean ± SD. $^*p < 0.05$ vs the Control group. $^{\#}p < 0.05$ vs the CUMS group. $^{@}p < 0.05$ vs the LV-NC group. $^{\&}p < 0.05$ vs the CUMS+JuA group.

Abbreviations: CUMS, chronic unpredictable mild stress; CUMS+JuA, CUMS treated with JuA at 50 mg/kg; CUMS+JuA+Sham, CUMS treated with JuA at 50 mg/kg but subjected to a sham procedure; LV-NC-RNAi/LV-NC, lentiviral vector normal control shRNA; LV-Shh-RNAi/LV-Shh, lentiviral vector expressing Shh shRNA; DAPI, 4',6-diamidino-2-phenylindole; DCX, doublecortin; Gli1, Gli family zinc finger 1; Gli2, Gli family zinc finger 2.

vHip plays a crucial role in motivation, social competence, and emotional behaviors associated with anxiety, frustration, and depression.[36] Studies have linked vHip to motivation, social interaction, lack of pleasure, despairing behaviors, anxiety, sleep, and eating.[37] The hippocampal dentate gyrus is a key region in synaptic circuits associated with emotion and memory functions, which is also a major site of neurogenesis with immature neurons are continually produced. New-born neurons remain in an immature state for an extended period before integrating into the adult circuitry.[38] DCX is a marker for immature neurons, and BrdU/DCX labeling is commonly used to quantify the number of these cells.[39] The experimental results indicate that pretreatment with JuA can significantly increase the number of immature neurons in the vDG. Shh, a secreted protein critical for immature neurons and its neuroplasticity,[40] exhibited significantly increasing in the vDG of CUMS rats after being treated with JuA, along with its downstream effectors Gli1 and Gli2. Therefore, we postulate that JuA increases the abundance of immature neurons in the vDG by upregulating Shh. To investigate the role of Shh in JuA's therapeutic effect, we employed LV-Shh-RNAi viruses to knock down Shh in the vDG of rats. We observed that Shh knockdown not only induced depressive-like behaviors (lack of pleasure, appetite loss, hopelessness, and learning memory deficits) but also reduced the abundance of immature neurons in rats given JuA treatment. These findings strongly suggest that JuA's antidepressant effects are mediated by Shh signaling.

In blood and cerebrospinal fluid, Ca^{2+} levels were elevated in depressed patients compared to healthy controls, which is consistent with elevated hippocampal Ca^{2+} levels in CUMS model rats, suggesting that calcium homeostatic dysregulation is present in depression.[41] Imbalances in calcium homeostasis can alter neuronal structure and function, potentially leading to irreversible neuronal damage. While the mechanisms are less well-studied in depression, dysregulation of calcium homeostasis in neurons is strongly implicated in many central nervous system diseases, including Alzheimer's and Parkinson's diseases.[42,43] CaMKII is the major calcium-regulated protein in neurons, suggesting it is a major target of calcium homeostatic dysregulation.[44] Immunofluorescence and calcium content assays showed that calcium homeostasis was dysregulated in immature neurons of the CUMS group, and JuA treatment maintained calcium homeostasis in immature neurons. However, the knockdown of Shh eliminated the protective effect of JuA. Furthermore, it has been shown that sustained neuronal activation depends on calcium homeostasis maintenance.[45] The hallmark of neuronal activation is C-fos, a calcium-dependent immediate-early gene and a regulator mediating neuronal excitability and survival. Our research confirmed that JuA ameliorated CUMS-induced inhibition of activity in immature neurons, whereas this effect did not occur after administration of LV-Shh-RNAi virus to knock down Shh. This result also indirectly confirms that JuA regulates the calcium homeostasis of immature neurons through Shh signaling.

Structural synaptic plasticity is a prerequisite for immature neurons integrate into established neural networks, involving changes in axons, dendrites, and dendritic spines.[46] Dendritic spines are highly dynamic, and changes in their density, size, and shape underlie structural synaptic plasticity in cognition and memory.[47] Golgi staining showed that the length, density, and complexity (represented by dendritic crossings) of dendrites were reduced in CUMS rats, which is consistent with previous results.[48] It was shown that the knockdown of Shh by viral injection blocked the protective effect of JuA on dendritic spine morphology in CUMS rats. PSD-95, as an important factor in synaptic plasticity and postsynaptic membrane stabilization, and Syn, as a marker of synaptic development and activity, are both major proteins involved in synaptic structural plasticity.[49] Immunofluorescence and immunoblotting results showed that the knockdown of Shh blocked the effects of JuA on PSD-95 and Syn. Taken together, our findings suggest that JuA can improve synaptic structural plasticity by altering dendritic spine morphology and regulating synaptic proteins.

Increased intracellular calcium levels activate CaMKII, triggering molecular events associated with synaptic structural plasticity, such as actin cytoskeleton remodeling and sporogenesis. At low Ca^{2+} concentrations, actin binds to CaMKII. When Ca^{2+} concentration increases, CaMKII dissociates from actin, opening a window for actin remodeling.[50] More importantly, calcium homeostasis in neurons regulates postsynaptic AMPAR content by affecting calmodulin binding to PSD-95. Further, AMPAR modulates the down- or up-regulation of postsynaptic strength, which is essential for synaptic homeostasis.[51] The relevance of synaptic structure can directly affect synaptic homeostasis.[52] In summary, JuA treatment may exert antidepressant-like effects by maintaining synaptic homeostasis through modulation of calcium homeostasis and synaptic structural plasticity.

In conclusion, JuA could alleviate the emotional behavior of CUMS rats, and the mechanism is related to mediating the calcium homeostasis and synaptic structural plasticity in immature neurons of vDG, through activation of the Shh

pathway targeting the Gli1/Gli2. JuA demonstrates potential as a natural, safe, and effective antidepressant. However, our limitations of study include the use of a single animal model. To address this, we will extract primary immature neuronal cells from the vHip of fetal rats for further validation. Moreover, advanced animal models, such as the primate tree shrew, are necessary for in-depth elucidation of JuA's therapeutic effects.

Conclusion

Our study suggests that JuA could be a promising therapeutic agent for mitigating CUMS-induced depressive-like behaviors. We hypothesize that its mechanism of action involves modulating calcium homeostasis and synaptic structural plasticity in immature neurons via the Shh signaling pathway. These findings elucidate a potentially novel neuroprotective mechanism of JuA for the treatment of depression and provide a strong theoretical basis for its use as a highly promising antidepressant drug.

Funding

This work was supported by the National Natural Science Foundation of China (No. 82474468), the Science and Technology Innovation Program of Hunan Province (No. 2024RC3200), the Scientific Research Project of Hunan Provincial Department of Education (No. 23A0281), the Open Fund for Chinese Medicine Powder and Innovative Drugs in the Cultivation Base of the Provincial-Ministry Jointly Established State Key Laboratory of Chinese Medicine (No. 23PTKF1013), the Training Plan of Outstanding Innovative Youth of Changsha (No. kq2009018), Scientific Research Projects of Chinese Medicine in Hunan Province (No. B2023021), Innovative Projects for Graduate Students of Hunan University of Traditional Chinese Medicine (No. 2024CX079), National Natural Science Foundation of China (No. 82104793), Hunan Provincial Natural Science Foundation of China (No. 2022JJ30451), and Hunan Youth Science and Technology Talent Project (No. 2022RC1226).

Disclosure

The authors report no conflicts of interest in this work.

References

1. Malhi GS, Mann JJ. Depression. *Lancet*. 2018;392(10161):2299–2312. doi:10.1016/S0140-6736(18)31948-2
2. Wang X, Li S, Yu J, et al. Saikosaponin B2 ameliorates depression-induced microglia activation by inhibiting ferroptosis-mediated neuroinflammation and ER stress. *J Ethnopharmacol*. 2023;316:116729. doi:10.1016/j.jep.2023.116729
3. Dioli C, Patrício P, Sousa N, et al. Chronic stress triggers divergent dendritic alterations in immature neurons of the adult hippocampus, depending on their ultimate terminal fields. *Transl Psychiatry*. 2019;9(1):143. doi:10.1038/s41398-019-0477-7
4. Rawat R, Tunc-Ozcan E, Dunlop S, et al. Ketamine's rapid and sustained antidepressant effects are driven by distinct mechanisms. *Cell Mol Life Sci*. 2024;81(1):105. doi:10.1007/s00018-024-05121-6
5. Workman JL, Chan MY, Galea LA. Prior high corticosterone exposure reduces activation of immature neurons in the ventral hippocampus in response to spatial and nonspatial memory. *Hippocampus*. 2015;25(3):329–344. doi:10.1002/hipo.22375
6. Griffioen G. Calcium Dyshomeostasis Drives Pathophysiology and Neuronal Demise in Age-Related Neurodegenerative Diseases. *Int J Mol Sci*. 2023;24(17):13243. doi:10.3390/ijms241713243
7. Sabti M, Sasaki K, Gadhi C, Isoda H. Elucidation of the Molecular Mechanism Underlying Lippia citriodora(Lim.)-Induced Relaxation and Anti-Depression. *Int J Mol Sci*. 2019;20(14):3556. doi:10.3390/ijms20143556
8. Yan Y, Xu X, Chen R, et al. Down-regulation of MST1 in hippocampus protects against stress-induced depression-like behaviours and synaptic plasticity impairments. *Brain Behav Immun*. 2021;94:196–209. doi:10.1016/j.bbi.2021.02.007
9. Zhu W, Zhang W, Yang F, et al. Role of PGC-1α mediated synaptic plasticity, mitochondrial function, and neuroinflammation in the antidepressant effect of Zi-Shui-Qing-Gan-Yin. *Front Neurol*. 2023;14:1108494. doi:10.3389/fneur.2023.1108494
10. Leem Y-H, Yoon -S-S, Jo SA. Imipramine Ameliorates Depressive Symptoms by Blocking Differential Alteration of Dendritic Spine Structure in Amygdala and Prefrontal Cortex of Chronic Stress-Induced Mice. *Biomol Ther*. 2020;28(3):230–239. doi:10.4062/biomolther.2019.152
11. Briscoe J, Small S. Morphogen rules: design principles of gradient-mediated embryo patterning. *Development*. 2015;142(23):3996–4009. doi:10.1242/dev.129452
12. Luo Y, Wang Y, Qiu F, et al. Ablated Sonic Hedgehog Signaling in the Dentate Gyrus of the Dorsal and Ventral Hippocampus Impairs Hippocampal-Dependent Memory Tasks and Emotion in a Rat Model of Depression. *Mol Neurobiol*. 2023. doi:10.1007/s12035-023-03796-9
13. Briscoe J, Thérond PP. The mechanisms of Hedgehog signalling and its roles in development and disease. *Nat Rev Mol Cell Biol*. 2013;14(7):416–429. doi:10.1038/nrm3598
14. Petralia RS, Wang YX, Mattson MP, Yao PJ. Subcellular distribution of patched and smoothened in the cerebellar neurons. *Cerebellum*. 2012;11(4):972–981. doi:10.1007/s12311-012-0374-6

15. Liu Z, Zhao X, Liu B, et al. Jujuboside A, a neuroprotective agent from semen Ziziphi Spinosae ameliorates behavioral disorders of the dementia mouse model induced by Aβ 1-42. *Eur J Pharmacol*. 2014;738:206–213. doi:10.1016/j.ejphar.2014.05.041
16. Wang M XX, GI XJB, Pang GC. Influence of JuA in evoking communication changes between the small intestines and brain tissues of rats and the GABAA and GABAB receptor transcription levels of hippocampal neurons. *J Ethnopharmacol*. 2015;159:215–223. doi:10.1016/j.jep.2014.11.012
17. Han D, Wan C, Liu F, Xu X, Jiang L, Xu J. Jujuboside A Protects H9C2 Cells from Isoproterenol-Induced Injury via Activating PI3K/Akt/mTOR Signaling Pathway. *Evid Based Complement Alternat Med*. 2016;2016:9593716. doi:10.1155/2016/9593716
18. Li H, Li J, Zhang T, Xie X, Gong J. Antidepressant effect of Jujuboside A on corticosterone-induced depression in mice. *Biochem Biophys Res Commun*. 2022;620:56–62. doi:10.1016/j.bbrc.2022.06.076
19. Wang C, Chen JC, Xiao HH, et al. Jujuboside a promotes proliferation and neuronal differentiation of APPswe-overexpressing neural stem cells by activating Wnt/β-catenin signaling pathway. *Neurosci Lett*. 2022;772:136473. doi:10.1016/j.neulet.2022.136473
20. Deng D, Cui Y, Gan S, et al. Sinisan alleviates depression-like behaviors by regulating mitochondrial function and synaptic plasticity in maternal separation rats. *Phytomedicine*. 2022;106:154395. doi:10.1016/j.phymed.2022.154395
21. Yang YY, Deng RR, Xiang DX. Naodesheng Pills Ameliorate Cerebral Ischemia Reperfusion-Induced Ferroptosis via Inhibition of the ERK1/2 Signaling Pathway. *Drug Des Devel Ther*. 2024;18:1499–1514. doi:10.2147/DDDT.S443479
22. Zhang D, Guo Y, Wang Y. Immunomodulatory Effect of a New Ingredients Group Extracted from Astragalus Through Membrane Separation Technique. *Drug Des Devel Ther*. 2021;15:1595–1607. doi:10.2147/DDDT.S309422
23. Teng Y, Zhang J, Zhang Z, Feng J. The Effect of Chronic Fluorosis on Calcium Ions and CaMKIIα, and c-fos Expression in the Rat Hippocampus. *Biol Trace Elem Res*. 2018;182(2):295–302. doi:10.1007/s12011-017-1098-8
24. Wang YJ, Chan MH, Chen L, Wu SN, Chen HH. Resveratrol attenuates cortical neuron activity: roles of large conductance calcium-activated potassium channels and voltage-gated sodium channels. *J Biomed Sci*. 2016;23(1):47. doi:10.1186/s12929-016-0259-y
25. Silva-Peña D, Rivera P, Alén F, et al. Oleoylethanolamide Modulates BDNF-ERK Signaling and Neurogenesis in the Hippocampi of Rats Exposed to Δ(9)-THC and Ethanol Binge Drinking During Adolescence. *Front Mol Neurosci*. 2019;12:96. doi:10.3389/fnmol.2019.00096
26. Empana JP, Boutouyrie P, Lemogne C, Jouven X, van Sloten TT. Microvascular Contribution to Late-Onset Depression: mechanisms, Current Evidence, Association With Other Brain Diseases, and Therapeutic Perspectives. *Biol Psychiatry*. 2021;90(4):214–225. doi:10.1016/j.biopsych.2021.04.012
27. Caldwell DM, Davies SR, Hetrick SE, et al. School-based interventions to prevent anxiety and depression in children and young people: a systematic review and network meta-analysis. *Lancet Psychiatry*. 2019;6(12):1011–1020. doi:10.1016/S2215-0366(19)30403-1
28. Shi ZM, Jing JJ, Xue ZJ, et al. Stellate ganglion block ameliorated central post-stroke pain with comorbid anxiety and depression through inhibiting HIF-1α/NLRP3 signaling following thalamic hemorrhagic stroke. *J Neuroinflammation*. 2023;20(1):82. doi:10.1186/s12974-023-02765-2
29. Liu MY, Yin CY, Zhu LJ, et al. Sucrose preference test for measurement of stress-induced anhedonia in mice. *Nat Protoc*. 2018;13(7):1686–1698. doi:10.1038/s41596-018-0011-z
30. Camargo A, Pazini FL, Rosa JM, et al. Augmentation effect of ketamine by guanosine in the novelty-suppressed feeding test is dependent on mTOR signaling pathway. *J Psychiatr Res*. 2019;115:103–112. doi:10.1016/j.jpsychires.2019.05.017
31. Amin F, Ibrahim M, Rizwan-Ul-Hasan S, et al. Interactions of Apigenin and Safranal with the 5HT1A and 5HT2A Receptors and Behavioral Effects in Depression and Anxiety: a Molecular Docking, Lipid-Mediated Molecular Dynamics, and In Vivo Analysis. *Molecules*. 2022;27(24):8658. doi:10.3390/molecules27248658
32. Tabassum S, Misrani A, Huo Q, Ahmed A, Long C, Yang L. Minocycline Ameliorates Chronic Unpredictable Mild Stress-Induced Neuroinflammation and Abnormal mPFC-HIPP Oscillations in Mice. *Mol Neurobiol*. 2022;59(11):6874–6895. doi:10.1007/s12035-022-03018-8
33. Vorhees CV, Williams MT. Morris water maze: procedures for assessing spatial and related forms of learning and memory. *Nat Protoc*. 2006;1(2):848–858. doi:10.1038/nprot.2006.116
34. Hernández-Mercado K, Zepeda A. Morris Water Maze and Contextual Fear Conditioning Tasks to Evaluate Cognitive Functions Associated With Adult Hippocampal Neurogenesis. *Front Neurosci*. 2021;15:782947. doi:10.3389/fnins.2021.782947
35. Qian H, Shu C, Xiao L, Wang G. Histamine and histamine receptors: roles in major depressive disorder. *Front Psychiatry*. 2022;13:825591. doi:10.3389/fpsyt.2022.825591
36. Bassett B, Subramaniyam S, Fan Y, et al. Minocycline alleviates depression-like symptoms by rescuing decrease in neurogenesis in dorsal hippocampus via blocking microglia activation/phagocytosis. *Brain Behav Immun*. 2021;91:519–530. doi:10.1016/j.bbi.2020.11.009
37. Yoshida K, Drew MR, Mimura M, Tanaka KF. Serotonin-mediated inhibition of ventral hippocampus is required for sustained goal-directed behavior. *Nat Neurosci*. 2019;22(5):770–777. doi:10.1038/s41593-019-0376-5
38. Ghibaudi M, Amenta A, Agosti M, et al. Consistency and Variation in Doublecortin and Ki67 Antigen Detection in the Brain Tissue of Different Mammals, including Humans. *Int J Mol Sci*. 2023;24(3):2514. doi:10.3390/ijms24032514
39. Patkar OL, Belmer A, Beecher K, Jacques A, Bartlett SE. Pindolol Rescues Anxiety-Like Behavior and Neurogenic Maladaptations of Long-Term Binge Alcohol Intake in Mice. *Front Behav Neurosci*. 2019;13:264. doi:10.3389/fnbeh.2019.00264
40. Li J, Li C, Subedi P, et al. Light Alcohol Consumption Promotes Early Neurogenesis Following Ischemic Stroke in Adult C57BL/6J Mice. *Biomedicines*. 2023;11(4):1074. doi:10.3390/biomedicines11041074
41. Meng Y, Liu S, Yu M, et al. The Changes of Blood and CSF Ion Levels in Depressed Patients: a Systematic Review and Meta-analysis. *Mol Neurobiol*. 2024. doi:10.1007/s12035-023-03891-x
42. Overk C, Masliah E. Perspective on the calcium dyshomeostasis hypothesis in the pathogenesis of selective neuronal degeneration in animal models of Alzheimer's disease. *Alzheimers Dement*. 2017;13(2):183–185. doi:10.1016/j.jalz.2017.01.005
43. Glaser T, Arnaud Sampaio VF, Lameu C, Ulrich H. Calcium signalling: a common target in neurological disorders and neurogenesis. *Semin Cell Dev Biol*. 2019;95:25–33. doi:10.1016/j.semcdb.2018.12.002
44. Sałaciak K, Koszałka A, Żmudzka E, Pytka K. The Calcium/Calmodulin-Dependent Kinases II and IV as Therapeutic Targets in Neurodegenerative and Neuropsychiatric Disorders. *Int J Mol Sci*. 2021;22(9):4307. doi:10.3390/ijms22094307
45. Chamaa F, Darwish B, Arnaout R, et al. Sustained Activation of the Anterior Thalamic Neurons with Low Doses of Kainic Acid Boosts Hippocampal Neurogenesis. *Cells*. 2022;11(21):3413. doi:10.3390/cells11213413
46. Kochan S, Malo MC, Jevtic M, et al. Enhanced mitochondrial fusion during a critical period of synaptic plasticity in adult-born neurons. *Neuron*. 2024;112(12):1997–2014.e6. doi:10.1016/j.neuron.2024.03.013

47. Mu L, Cai J, Gu B, et al. Treadmill Exercise Prevents Decline in Spatial Learning and Memory in 3×Tg-AD Mice through Enhancement of Structural Synaptic Plasticity of the Hippocampus and Prefrontal Cortex. *Cells*. 2022;11(2):244. doi:10.3390/cells11020244
48. Meng P, Zhang X, Liu TT, et al. A whole transcriptome profiling analysis for antidepressant mechanism of Xiaoyaosan mediated synapse loss via BDNF/trkB/PI3K signal axis in CUMS rats. *BMC Complement Med Ther*. 2023;23(1):198. doi:10.1186/s12906-023-04000-0
49. Sadigh-Eteghad S, Geranmayeh MH, Majdi A, Salehpour F, Mahmoudi J, Farhoudi M. Intranasal cerebrolysin improves cognitive function and structural synaptic plasticity in photothrombotic mouse model of medial prefrontal cortex ischemia. *Neuropeptides*. 2018;71:61–69. doi:10.1016/j.npep.2018.07.002
50. Yasuda R, Hayashi Y, Hell JW. CaMKII: a central molecular organizer of synaptic plasticity, learning and memory. *Nat Rev Neurosci*. 2022;23(11):666–682. doi:10.1038/s41583-022-00624-2
51. Chowdhury D, Turner M, Patriarchi T, et al. Ca(2+)/calmodulin binding to PSD-95 mediates homeostatic synaptic scaling down. *EMBO J*. 2018;37(1):122–138. doi:10.15252/embj.201695829
52. Moulin TC, Rayêe D, Schiöth HB. Dendritic spine density changes and homeostatic synaptic scaling: a meta-analysis of animal studies. *Neural Regen Res*. 2022;17(1):20–24. doi:10.4103/1673-5374.314283